Available online at www.sciencedirect.com
ScienceDirect
Trans. Nonferrous Met. Soc. China 31(2021) 2128−2138
Transactions of Nonferrous Metals Society of China
www.tnmsc.cn

Influence of high concentration Zn^{2+} on floatability of sphalerite in acidic system

Ting-sheng QIU[1], Guo-dong LI[1,2], Xiao-bo LI[1], Hua-shan YAN[1], Chen LIU[1]

1. School of Resource and Environmental Engineering, Jiangxi University of Science and Technology, Ganzhou 341000, China;
2. Northwest Research Institute of Mining and Metallurgy, Baiyin 730900, China

Received 15 April 2020; accepted 30 April 2021

Abstract: The influence of high concentration Zn^{2+} on the floatability of sphalerite in an acidic system was investigated via flotation experiments, zeta potential measurements, contact angle measurements, and X-ray photoelectron spectroscopy. The results indicated that Zn^{2+} was adsorbed on the sphalerite surface and a Zn-hydroxyl complex was formed at a pH of 4 and a Zn^{2+} concentration of 4×10^{-2} mol/L. The zeta potential increased and the contact angle decreased from 84.80° to 36.48°, strongly inhibiting the floatability of sphalerite. When S^{2-} or Cu^{2+} activator was used alone, sphalerite was not activated after Zn^{2+} was adsorbed, and its contact angle did not change significantly. However, by using a combination of S^{2-} and Cu^{2+} activators, its floatability was realized after Zn^{2+} adsorption. This result was attributed to the removal of the Zn-hydroxyl complex on the surface of sphalerite by S^{2-}. After this removal, Cu^{2+} was adsorbed on the sphalerite surface to form a $Cu_2S{\cdot}S^0$ hydrophobic film.
Key words: acidic system; high concentration Zn^{2+}; sphalerite; flotation

1 Introduction

Sphalerite, a common zinc mineral, is the main raw material for zinc smelting. Zinc metal production usually begins with the recovery of sphalerite concentrate from ore by flotation, followed by the process of "roasting−acid leaching–purification–electrodeposition" [1,2]. A small amount of sphalerite is left in the leaching residue produced by zinc hydrometallurgy [3,4]. In addition to hydrometallurgical recovery and pyrometallurgical recovery [5−9], flotation is also an important method for recovering valuable metals from zinc leaching residues [10]. Sulfuric acid is used as the leaching agent for the roasted zinc sulfide product. Sulfuric acid and Zn^{2+} remain in the zinc leaching residues from different thickening and filtration stages of zinc hydrometallurgy. Thus, the pulp has generally a pH between 3 and 5 and contains a Zn^{2+} high concentration during the pulping and flotation of sphalerite from zinc leaching residues. Sodium hydroxide or calcium oxide is usually not used to improve the pH of the pulp before the flotation of sphalerite from zinc leaching residues. This is primarily because a large amount of reagent is required for adjusting the pH value of the pulp to an alkaline value, which increases the beneficiation cost. Moreover, large amount of gold, silver, and other associated precious metals are present in the zinc leaching residues. However, a high pH inhibits the flotation of gold and silver, which is not conducive to the full recovery of valuable metals in the residues. Mineralogical research on zinc leaching residues indicates that most of the zinc in the residues is in the form of sphalerite, zinc sulfate, zinc ferrite, and zinc silicate, and sphalerite is the major recovered

Corresponding author: Guo-dong LI, Tel: +86-797-8312759, E-mail: lgdabcd@163.com
DOI: 10.1016/S1003-6326(21)65643-1

material [2,11,12].

Cu^{2+} is widely used as an activation ion for sphalerite. Under alkaline conditions, Cu^{2+} is adsorbed on the sphalerite surface in the form of Cu^{2+} or $Cu(OH)_2$ and interacts with Zn^{2+} in the sphalerite lattice to form copper sulfide, polysulfide, and elemental sulfur to activate sphalerite [13,14]. ANDER et al [15] studied the mechanism of sphalerite activation by Cu^{2+} at a high pH and proposed a model for surface adsorption. According to ALBRECHT et al [16], the mechanism of sphalerite activation by Cu^{2+} in alkaline environments is that Cu^{2+} is adsorbed on the surface of sphalerite to complete a one-to-one zinc–copper exchange and form copper sulfide and polysulfide/elemental sulfur, as shown in Reactions. (1)−(4):

In basic medium:

$$ZnS+Cu(OH)_2 \rightleftharpoons ZnS–Cu(OH)_2 \quad (1)$$

$$ZnS−Cu(OH)_2 \rightleftharpoons CuS+Zn(OH)_2 \quad (2)$$

In acidic medium:

$$ZnS+Cu^{2+} \rightleftharpoons ZnS−Cu^{2+} \quad (3)$$

$$ZnS−Cu^{2+} \rightleftharpoons CuS+Zn^{2+} \quad (4)$$

The CuS generated on the sphalerite would be further transformed into Cu_2S and elemental sulfur with Reaction (5):

$$2CuS \rightleftharpoons Cu_2S+S^0 \quad (5)$$

(with S_n^{2-} as an intermediate oxidation product)

Generally, sphalerite has good floatability at a low pH and exhibits a high recovery rate even when Cu^{2+} is not activated [17,18]. However, in actual zinc leaching residue flotation in industrial production where the acidic pulp contains a large amount of Zn^{2+}, sphalerite recovery from the leaching residue via direct flotation or activated flotation is difficult when Cu^{2+} is used alone. Effective sphalerite activation can be achieved only when appropriate amount of Na_2S and $CuSO_4$ are added simultaneously. This phenomenon is due to the high concentration of Zn^{2+} in the pulp, which interacts with sulfate to form $ZnSO_4$ and replaces the active metal ions on the mineral surface under specific pulp conditions; consequently, a hydrophilic zinc hydroxy film is formed on the surface of sphalerite, which inhibits its floatability. Most researchers believe that sphalerite is inhibited by zinc salts in alkaline environments because of the formation of zinc hydroxide on the surface of sphalerite [18−21]. However, only a few experimental and theoretical studies have explored the problem of strong sphalerite inhibition in acidic pulp containing large amount of Zn^{2+} and the difficulty of achieving direct or activated flotation using Cu^{2+} alone. The addition of an appropriate amount of a combined activator, i.e., Na_2S and $CuSO_4$, can effectively activate sphalerite. The inhibition mechanism of Zn^{2+} on sphalerite in acidic pulp and the activation mechanism of sphalerite after addition of a combined activator (Cu^{2+} and $S^{2−}$) should be further analyzed through testing and experimental verification.

In this study, using sphalerite as the research object, the influence of high concentration Zn^{2+} on the flotation behavior of sphalerite and the mechanism of activating the suppressed sphalerite with a combination of Cu^{2+} and $S^{2−}$ activators were investigated through mono-mineral flotation experiments, zeta potential measurements, contact angle measurements, and X-ray photoelectron spectroscopy (XPS) in an acidic environment with a pH of 4. This research provides a theoretical basis for recovering sphalerite from leaching residues via direct activation flotation.

2 Experimental

2.1 Materials and reagents

A pure sphalerite sample was collected from a lead–zinc ore in Guanxi, China. Elemental analysis indicated that the sample had 66.20 wt.% Zn and 32.40 wt.% S with a purity above 98%. The X-ray diffraction spectrum of the sample is shown in Fig. 1. The sphalerite samples were processed into powder and block samples. The particle size of the powder samples was 45−74 μm, and that of the block samples was approximately 200 μm. Analytical grade H_2SO_4 was used as the pH-controlling agent, while analytical grade $CuSO_4$ and Na_2S were utilized as activators. Analytical grade $ZnSO_4$ was employed as a modifier for sphalerite. Industrial grade ammonium dibutyl dithiophosphate (ADD) was used as a collector, and deionized water was applied in all experiments.

Sphalerite after the adsorption of $ZnSO_4$ was labeled as sphalerite−Zn^{2+}, whereas sphalerite activated by $CuSO_4$ alone was labeled as sphalerite−Cu^{2+}. Sphalerite−Zn^{2+} samples activated by $CuSO_4$ alone, Na_2S alone, and a combination of $CuSO_4$ and Na_2S were labeled as sphalerite−

Zn^{2+}–Cu^{2+}, sphalerite–Zn^{2+}–S^{2-}, and sphalerite–Zn^{2+}–Cu^{2+}–S^{2-}, respectively.

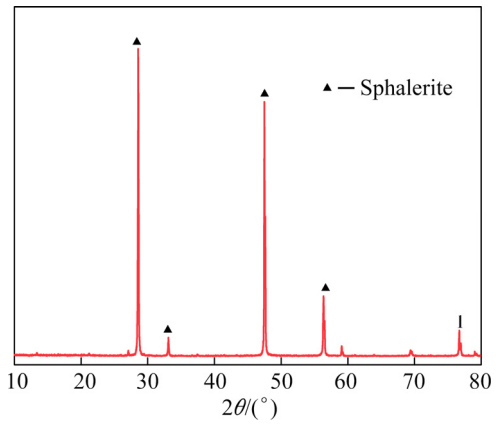

Fig. 1 X-ray diffraction spectrum of sphalerite sample

2.2 Flotation experiments

Mono-mineral flotation experiments were performed in an XFGCII hanging trough machine with a 25 mL flotation cell at an impeller speed of 1800 r/min. Firstly, 3 g of the pure sphalerite sample was ultrasonically cleaned for 5 min. Then, deionized water was added to the flotation cell for pulp conditioning. Subsequently, size mixing was conducted, followed by (1) addition of sulfuric acid to adjust the pH to 4; (2) addition of $ZnSO_4$ solution (1×10^{-2} mol/L) and stirring for 5 min; (3) addition of the activator (2×10^{-4} mol/L Cu^{2+}), collector (2×10^{-5} mol/L ADD), and stirring for 2 min; (4) flotation and scraping of bubbles for 4 min; (5) filtering and drying of the foam products and products in the cell; (6) calculation of the recovery rate after weighing and recording. The recovery rate (ε) of sphalerite was calculated using the following formula:

$$\varepsilon=\frac{m_1}{m_1+m_2} \tag{6}$$

where m_1 and m_2 are the masses of the flotation and bottom products, respectively, after drying. The tests were duplicated, and the average recovery rate was reported together with the error bars of the 95% confidence interval of a Student's t-distribution.

2.3 Surface zeta potential measurements

The zeta potential of the sphalerite surface was measured using a zeta potential analyzer (Zetasizer Nano Zs90). Before the measurements, sphalerite was ground to 5 μm in an agate mortar. Then, pulp with a content of 0.01 wt.% was prepared in a beaker, and its pH was adjusted using H_2SO_4. The reagents were added according to the order of the flotation experiments, and the mixture was blended using a magnetic stirrer for 5 min. The suspension was allowed to settle for 10 min with stirring. Afterward, the supernatant suspension of sphalerite was obtained to measure the zeta potential before and after the interaction between the minerals and reagents. Zeta potential measurements were performed in duplicate, and the average value of the measurements was reported together with the error bars of a 95% confidence interval of a Student's t-distribution.

2.4 Contact angle measurements

The wetting contact angle of the mineral surface was determined using an automatic surface tension meter (K100C, Germany). Before measuring the contact angle, the pure mineral block was cut and polished into a 10 mm × 20 mm × 10 mm smooth rectangular prism. The surface was finely ground with a metallographic sandpaper and cleaned ultrasonically for 5 min. Afterward, the pH of the pulp was adjusted to a set value. Different reagents were added as required, and the mixture was stirred for 10 min. The contact angle (θ) was measured after stirring. Seven points were tested for each sample.

2.5 XPS tests

XPS tests were carried out using a multifunctional X-ray photoelectron spectrometer (ESCALAB MarkII, USA) equipped with an Al K_α X-ray source (1486.6 eV). The instrument was calibrated by the binding energy of C 1s (284.60 eV) with an error of ±0.3 eV. For the XPS tests, the powder samples reacted adequately in accordance with the designed solution conditions. The samples were filtered using a qualitative filter paper, washed repeatedly with deionized water, placed in a vacuum drying oven, dried at 80 °C, and tested afterward.

3 Results and discussion

3.1 Effect of Zn^{2+} concentration on flotation behavior of sphalerite

Figure 2(a) shows the effects of different Zn^{2+} concentrations on the flotation performance of sphalerite at a pH of 4 and an ADD concentration

of 2×10^{-5} mol/L. The flotation recovery rate of sphalerite reaches 96.2% in the absence of Zn^{2+}, indicating that sphalerite has good floatability even without the addition of any activator. This result is consistent with that of a previous study [17]. However, the flotation recovery rate of sphalerite significantly decreases with increasing Zn^{2+} concentration. When the concentration of Zn^{2+} reaches 4×10^{-2} mol/L, the recovery rate of sphalerite decreases to 55%, indicating that Zn^{2+} has a strong inhibitory effect on sphalerite flotation.

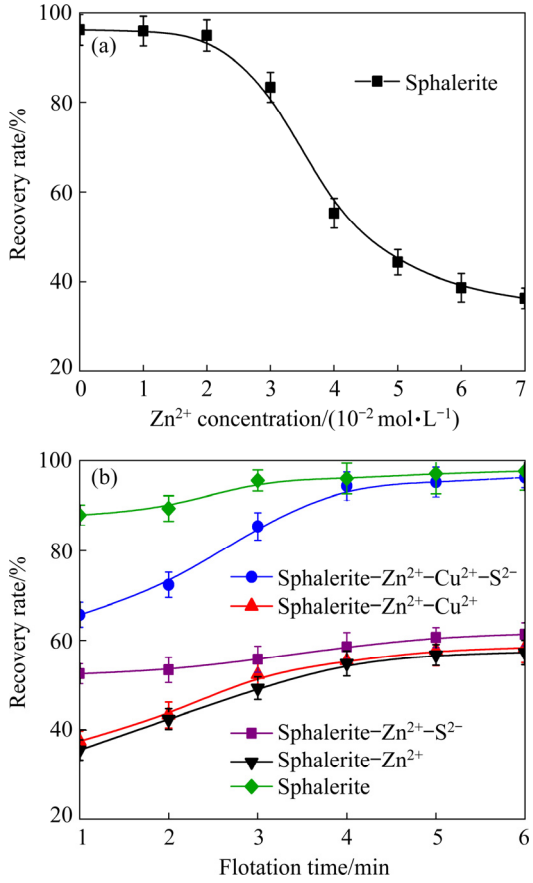

Fig. 2 Flotation recovery rates of sphalerite under different conditions: (a) Different Zn^{2+} concentrations; (b) Different ion combinations

Figure 2(b) illustrates the flotation recovery rate of sphalerite under different conditions as a function of flotation time at a pH of 4. The concentrations of Zn^{2+}, S^{2-}, Cu^{2+}, and ADD are 4×10^{-2}, 2×10^{-4}, 2×10^{-4}, and 2×10^{-5} mol/L, respectively. Sphalerite–Zn^{2+} cannot be activated effectively by a single activator such as Cu^{2+} or S^{2-} in the acidic system, and its flotation recovery rate does not exceed 60%. However, sphalerite−Zn^{2+} can be activated effectively by a combination of Cu^{2+} and S^{2-} activators, and the flotation recovery rate reaches 94.32%. Generally, Cu^{2+} can effectively activate sphalerite, but the experimental results show that the activation effect of Cu^{2+} is considerably reduced in the presence of Zn^{2+}. A possible explanation is that sphalerite reacts with Zn^{2+} and forms a zinc hydrophilic compound on the sphalerite surface, thus preventing Cu^{2+} from being adsorbed on the surface of sphalerite, which is consistent with a previous study [22]. The activation mechanism of sphalerite with Cu^{2+} in acidic media is described by the following reaction:

$$ZnS+Cu^{2+}\rightarrow CuS+Zn^{2+}\rightarrow 1/2Cu_2S+1/2S+Zn^{2+} \quad (7)$$

Similar to the process described in Reaction (5), the adsorption and incorporation of Cu^{2+} in the crystal network of sphalerite cause an oxidation–reduction reaction in which Cu^{2+} oxidizes the sulfide of the mineral. Consequently, it is reduced to Cu^{+}, yielding the final products of covellite (CuS), chalcocite (Cu_2S), and elemental sulfur, which are hydrophobic in nature. Based on the above results, it is inferred that Zn^{2+}, as a common ion added to the solution, decreases the solubility of sphalerite and is adsorbed on the surface as $ZnOH^{+}$, which inhibits Cu^{2+} adsorption, thus avoiding the conventional activation mechanism, which gives rise to the formation of hydrophobic species (Reactions (1)−(5)).

3.2 Zeta potential

Figure 3 shows the zeta potential of sphalerite under different ion combination conditions at pH 4, and Zn^{2+}, S^{2-}, and Cu^{2+} concentrations of 4×10^{-2}, 2×10^{-4}, and 2×10^{-4} mol/L, respectively. In the absence of Zn^{2+}, the zeta potential of sphalerite is (−22.31±1.02) mV, which is consistent with previously reported test data [23]. By contrast, the zeta potential increases to (−13.25±1.12) mV in the presence of Zn^{2+}, which may be attributed to Zn^{2+} adsorption that neutralizes the negative charge on the sphalerite surface. The addition of the Cu^{2+} activator significantly reduces the zeta potential of sphalerite to (−39.35±1.23) mV in the absence of Zn^{2+}, suggesting that Cu^{2+} is adsorbed on the sphalerite surface. CuS, Cu_2S, and $(Cu^{+})_2(S_2)^{2-}$ are probably formed on surface of sphalerite [23,24]. The zeta potential of sphalerite−Zn^{2+}−Cu^{2+} is (−15.27±0.93) mV, which is slightly different from that of sphalerite–Cu^{2+}, indicating that Cu^{2+} does not play an active role in the presence of Zn^{2+}. With the addition of S^{2-}, the surface zeta potential of

sphalerite−Zn^{2+}−S^{2-} becomes (−16.52±1.16) mV and exhibits a negative shift, indicating that S^{2-} is absorbed on the sphalerite–Zn^{2+} surface to neutralize the positive charge. When the combined activator of Cu^{2+} and S^{2-} is added to the pulp, the zeta potential of sphalerite−Zn^{2+}−Cu^{2+}–S^{2-} becomes (−35.36±1.07) mV, which is similar to that of sphalerite−Cu^{2+}. This result indicates that Cu^{2+} can be effectively adsorbed on the sphalerite−Zn^{2+} surface and can perform its activation effect in the presence of S^{2-}.

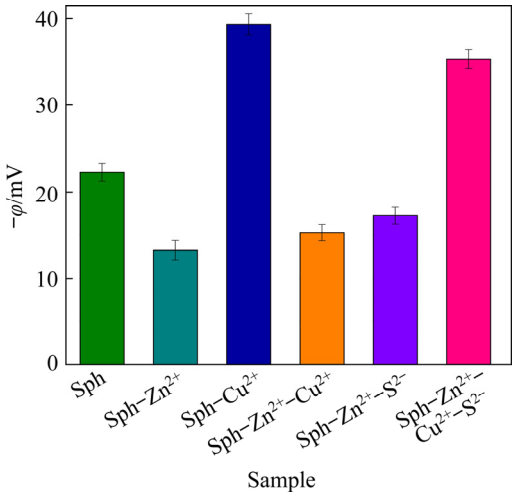

Fig. 3 Zeta potential (φ) of sphalerite (Sph) under different ion combination conditions

3.3 Contact angle

Figure 4 displays the contact angle of sphalerite under different ion combination conditions at pH 4, and Zn^{2+}, S^{2-}, and Cu^{2+} concentrations of 4×10^{-2}, 2×10^{-4}, and 2×10^{-4} mol/L, respectively. The contact angle of pure sphalerite is 84.80°, indicating that it has good floatability in the acidic system. In contrast, that of sphalerite−Zn^{2+} is significantly reduced to 36.48°, indicating a hydrophilic state. Without the addition of Zn^{2+}, the contact angle of sphalerite activated by Cu^{2+} is 90.40°, which indicates a hydrophobic state. The contact angles of sphalerite−Zn^{2+}−Cu^{2+} and sphalerite−Zn^{2+}−S^{2-} are 40.17° and 43.79°, respectively, indicating a hydrophilic state. Thus, a single activator cannot significantly improve the hydrophobicity of sphalerite−Zn^{2+}. However, when Cu^{2+} and S^{2-} are combined, the contact angle of sphalerite−Zn^{2+}−Cu^{2+}−S^{2-} increases to 102.29°, indicating a hydrophobic state and suggesting that the addition of a combined activator promotes the activation of sphalerite−Zn^{2+}.

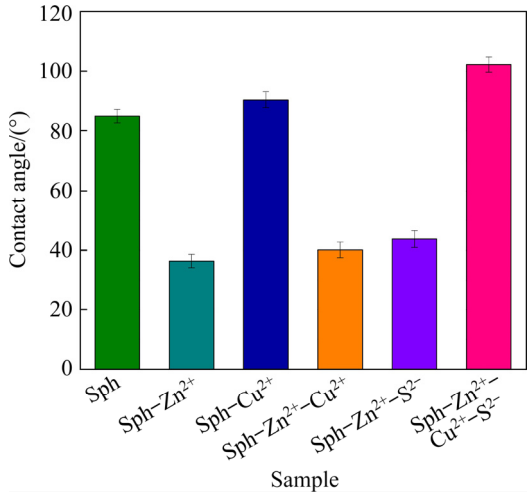

Fig. 4 Contact angle of sphalerite under different ion combination conditions

3.4 XPS spectra

3.4.1 Surface properties of sphalerite−Zn^{2+}

XPS analysis was conducted on pure sphalerite and sphalerite−Zn^{2+} at a pH of 4, and Zn^{2+} concentration of 4×10^{-2} mol/L to further ascertain the adsorption form of Zn^{2+} on the sphalerite surface.

Figure 5 shows that the binding energy of the photoelectron characteristic peaks of Zn 2p, S 2p, C 1s, and O 1s are 1021.96, 161.73, 284.78, and 531.65 eV, respectively, which are consistent with previous test data [14,25]. Figure 6 and Table 1 present the binding energies of Zn 2p and S 2p; the peak area and shape of sphalerite−Zn^{2+} are not significantly different from those of pure sphalerite, indicating that the states of Zn and S atoms are not changed during Zn^{2+} adsorption on sphalerite. However, the mole fraction of O 1s on sphalerite−

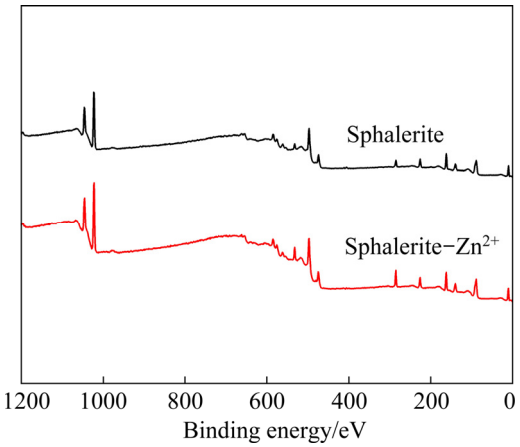

Fig. 5 XPS spectra of sphalerite before and after Zn^{2+} adsorption

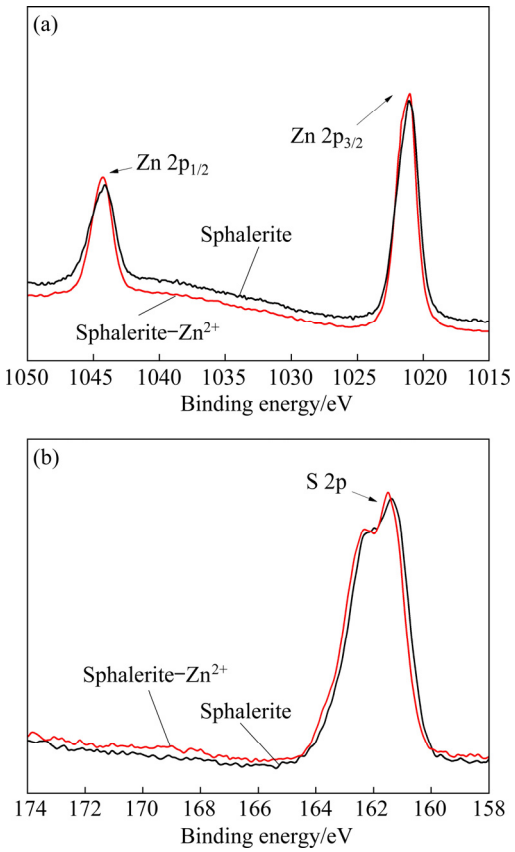

Fig. 6 Zn 2p (a) and S 2p (b) spectra of sphalerite before and after Zn^{2+} adsorption

Table 1 Binding energy and mole fraction of elements identified on sphalerite surface before and after Zn^{2+} adsorption

Sample	Atomic orbital	Binding energy/eV	Mole fraction/%
Sphalerite	S 2p	161.73	34.48
	C 1s	284.78	26.32
	O 1s	531.65	8.09
	Zn 2p	1021.96	31.11
Sphalerite−Zn^{2+}	S 2p	161.05	27.34
	C 1s	284.55	25.21
	O 1s	531.58	12.06
	Zn 2p	1021.69	35.39

Zn^{2+} is 12.06%, which is 3.97% higher than that on the pure sphalerite, indicating that O atoms may have participated in the Zn^{2+} adsorption reaction on sphalerite.

Figure 7 illustrates the narrow spectra of O 1s in sphalerite and sphalerite–Zn^{2+}. The peaks at 531.28 and 532.15 eV are attributed to the O 1s of OH^- from metal hydroxy complexes on the mineral surfaces and O 1s from the hydration layer on the mineral surface or water molecules on the sphalerite surface by chemical adsorption, respectively [26]. After the adsorption of Zn^{2+}, the peak of OH^- in the spectra of O 1s (531.49 eV) on sphalerite is enhanced, indicating that the proportion of OH^- on the surface of sphalerite increases (Figs. 7(a) and (b)).

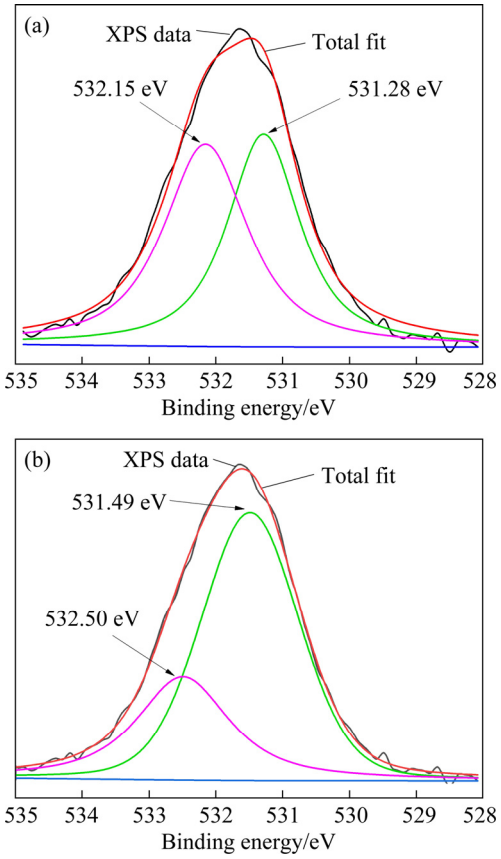

Fig. 7 O 1s spectra of sphalerite before (a) and after (b) Zn^{2+} adsorption

Table 2 presents the mole fractions and peak areas of the oxygen-containing compounds on the surfaces of sphalerite and sphalerite−Zn^{2+}. The proportions of hydroxyl complexes in the surface oxygen-containing compounds significantly increase on the surface of sphalerite−Zn^{2+}, with a mole fraction of 71.16%. Meanwhile, the mole fraction of the hydroxyl complexes in the oxygenated compounds on the surface of pure sphalerite is 44.04%. Zn^{2+} was absorbed on the surface of sphalerite in the form of a metal hydroxyl complex, which made the surface of sphalerite hydrophilic, reduced the floatability, and inhibited the recovery of sphalerite.

Table 2 O 1s species compositions of sphalerite before and after Zn^{2+} adsorption

Sample	Species	Binding energy/eV	Peak area (cps)	Mole fraction/%
Sphalerite	OH^-	531.33	4136.60	44.04
	H_2O	532.10	5409.71	57.76
Sphalerite–Zn^{2+}	OH^-	531.52	12083.33	71.16
	H_2O	532.34	5636.69	28.84

3.4.2 Surface properties of sphalerite−Zn^{2+}−Cu^{2+}

The reason for the fact that sphalerite–Zn^{2+} was difficult to activate by Cu^{2+} alone was determined by subjecting sphalerite−Cu^{2+} and sphalerite−Zn^{2+}−Cu^{2+} to XPS tests at a pH of 4. The details of the analysis are presented in Table 3.

Table 3 Binding energy and mole fraction of elements identified in Cu^{2+}-activated sphalerite before and after Zn^{2+} adsorption

Sample	Atomic orbital	Binding energy/eV	Mole fraction/%
Sphalerite−Cu^{2+}	S 2p	161.57	26.82
	C 1s	284.83	27.32
	O 1s	532.20	8.84
	Cu 2p	932.4	8.25
	Zn 2p	1021.67	28.77
Sphalerite−Zn^{2+}−Cu^{2+}	S 2p	161.62	27.56
	C 1s	284.79	28.32
	O 1s	532.36	11.36
	Cu 2p	932.18	2.14
	Zn 2p	1021.35	30.62

As shown in Table 3, the mole fractions of Cu 2p on the sphalerite–Cu^{2+} and sphalerite−Zn^{2+}−Cu^{2+} surfaces are 8.25% and 2.14%, respectively, indicating that Cu^{2+} is difficult to adsorb on the sphalerite−Zn^{2+} surface. The adsorption of Cu^{2+} on the sphalerite−Zn^{2+}−Cu^{2+} surface is mainly due to the combination reaction between Cu^{2+} and S atoms on the sphalerite surface.

The narrow spectra of S 2p on the surface of pure sphalerite and sphalerite−Zn^{2+}−Cu^{2+} were analyzed via peak fitting and separation to further examine the change in S valences (Fig. 8).

Figures 8(a) and (b) display two peaks of the S atoms in the spectra of pure sphalerite. The S $2p_{3/2}$ spectra with binding energies of 161.35 and 162.58 eV are attributed to S^{2-} and S_2^{2-} or metal-deficient sulfide on the sphalerite surface, respectively [27,28]. Two valence peaks of the S atoms are also observed in the spectra of sphalerite−Zn^{2+}−Cu^{2+}, and their binding energies are 161.36 and 162.54 eV, respectively. These values are consistent with the binding energies of the two valence states of the S atoms on the pure sphalerite surface, indicating that the valence state of the S atoms on the surface of sphalerite−Zn^{2+}−Cu^{2+} is not changed and Cu^{2+} is hardly adsorbed.

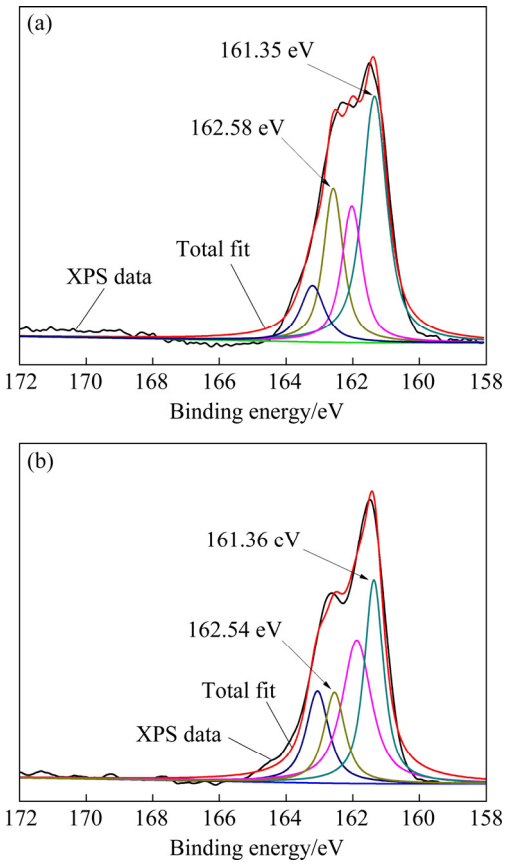

Fig. 8 S 2p spectra of sphalerite (a) and sphalerite−Zn^{2+}−Cu^{2+} (b)

3.4.3 Surface properties of sphalerite−Zn^{2+}−Cu^{2+}−S^{2-}

Figure 9 depicts the narrow spectra of S 2p on the surface of sphalerite−Cu^{2+} (Fig. 9(a)), sphalerite−Zn^{2+}−S^{2-} (Fig. 9(b)), and sphalerite−Zn^{2+}−Cu^{2+}−S^{2-} (Fig. 9(c)), which were analyzed via peak fitting and separation.

Figure 9(a) displays three peaks of the S atoms of the sphalerite−Cu^{2+} surface. The S $2p_{3/2}$ spectrum with a binding energy of 161.21 eV is assigned to S^{2-} in Zn−S on the sphalerite surface, and that with

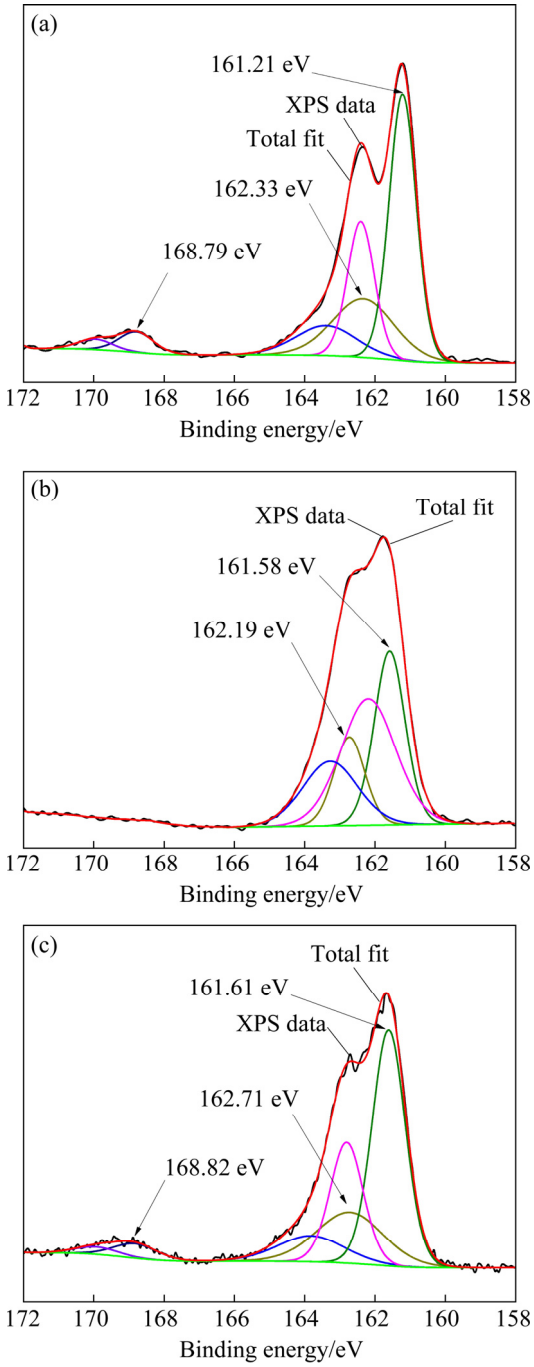

Fig. 9 S 2p spectra of sphalerite under different ion combination conditions: (a) Sphalerite−Cu^{2+}; (b) Sphalerite−Zn^{2+}−S^{2-}; (c) Sphalerite−Zn^{2+}−Cu^{2+}−S^{2-}

a binding energy of 162.33 eV is attributed to S_2^{2-} or metal-deficient sulfide. Sphalerite is activated by Cu^{2+} mainly because thermodynamically metastable copper(II)-substituted zinc sulfide phases may undergo a redox disproportion into either copper(I) sulfide and elemental sulfur ($Cu_2S{\cdot}S^0$) or copper(I) polysulfide (e.g., $(Cu^+)_2(S_2)^{2-}$) [23]. In addition, the S $2p_{3/2}$ spectrum with a binding energy of 168.79 eV is assigned to SO_4^{2-}, indicating that SO_4^{2-} is formed on the sphalerite surface during sphalerite activation by Cu^{2+}.

In Fig. 9(b), two peaks of the S atoms on the surface of sphalerite−Zn^{2+}−S^{2-} are shown in the spectra, and the binding energies are 161.58 eV and 162.19 eV respectively. They are assigned to S^{2-} in Zn−S on the sphalerite surface and S_2^{2-} or metal-deficient sulfide. Figures 8(a) and 9(b) also exhibit a small difference in the fitting results between sphalerite and sphalerite−Zn^{2+}−S^{2-}, indicating that the valence state of the S atoms in sphalerite−Zn^{2+}−S^{2-} is not changed. According to the results of the previous flotation experiments, Cu^{2+} can effectively activate sphalerite−Zn^{2+} when S^{2-} is added.

The valence states of the O atoms on the surface of sphalerite−Zn^{2+}−S^{2-} were analyzed via peak fitting and separation to further determine the effects of S^{2-} addition on the surface of sphalerite–Zn^{2+} (see Fig. 10 and Table 4). Figure 10 shows that the O atoms are absorbed on the surface of sphalerite−Zn^{2+}−S^{2-} in the form of OH^- and H_2O. The peaks at 531.31 and 532.32 eV are attributed to the O 1s of OH^- from metal hydroxyl complexes on the mineral surfaces and the O from the hydration layer on the mineral surface or water molecules on the sphalerite surface by chemical adsorption, respectively. The mole fractions of oxygen-containing compounds on the surface of sphalerite−Zn^{2+} are higher than those on sphalerite−Zn^{2+}− S^{2-}, with values of 71.16% (Table 2) and 46.75% (Table 4), respectively. This result indicates that the addition of S^{2-} can effectively reduce the content of the Zn-hydroxyl complex on the surface of the sphalerite.

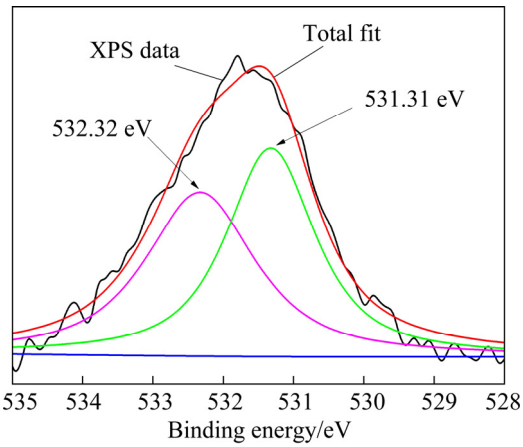

Fig. 10 O 1s spectra of sphalerite after Zn^{2+} adsorption by S^{2-} activation

Table 4 O 1s species compositions of sphalerite after Zn^{2+} adsorption by S^{2-} activation (sphalerite−Zn^{2+}−S^{2-})

Species	Binding energy/eV	Peak area (cps)	Mole fraction/%
OH^-	531.31	4614.85	46.75
H_2O	532.32	4480.73	53.25

Figure 9(c) illustrates the narrow spectra of S 2p on the surface of sphalerite−Zn^{2+}−Cu^{2+}−S^{2-} analyzed via peak fitting and separation. Three peaks of the S atom at 161.61, 162.71, and 168.82 eV, which are respectively assigned to S^{2-}, copper(I) sulfide and elemental sulfur ($Cu_2S{\cdot}S^0$) or copper(I) polysulfide (e.g., $(Cu^+)_2(S_2)^{2-}$), and SO_4^{2-} on sphalerite, are shown. These results are similar to the three valence states of the S atom on the surface of sphalerite−Cu^{2+}, indicating that the hydrophobic products formed on the surface of the three types of sphalerite are consistent. These can be verified further by the narrow spectral analysis of the Cu 2p of Cu atoms on the surfaces of sphalerite–Cu^{2+} and sphalerite−Zn^{2+}−Cu^{2+}−S^{2-} in Fig. 11.

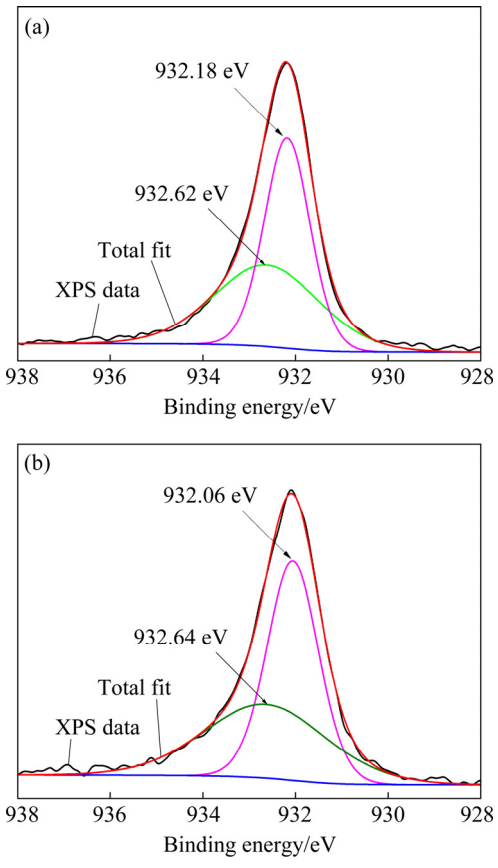

Fig. 11 Cu $2p_{2/3}$ spectra of sphalerite under different ion combination conditions: (a) Sphalerite−Cu^{2+}; (b) Sphalerite−Zn^{2+}−Cu^{2+}−S^{2-}

As displayed in Fig. 11(a), the peak at 932.62 eV is attributed to Cu^+ [29], indicating that Cu^{2+} activated the sphalerite in the acidic system in the form of Cu^+ species, that is, a $Cu_2S{\cdot}S^0$ hydrophobic film was formed on the sphalerite−Cu^{2+} surface [16]. Figure 11(b) shows that the same hydrophobic product is formed on the surface of sphalerite−Zn^{2+}−Cu^{2+}−S^{2-}.

4 Conclusions

(1) The mono-mineral flotation results indicated that a high concentration of Zn^{2+} at a pH of 4 strongly inhibited the sphalerite recovery. It was difficult to activate sphalerite−Zn^{2+} using a single activator (S^{2-} or Cu^{2+}), but effective activation was achieved with a recovery of 94.32% by a combination of S^{2-} and Cu^{2+} activators.

(2) The zeta potential and contact angle analyses revealed that the inhibiting effect of the high concentration Zn^{2+} was due to Zn^{2+} adsorption on the sphalerite surface, which resulted in an increased zeta potential and a decreased contact angle. When a single activator (Cu^{2+} or S^{2-}) was added, the zeta potential and contact angle of sphalerite−Zn^{2+} did not significantly change. However, effective activation of sphalerite−Zn^{2+} was realized by using a combination of Cu^{2+} and S^{2-} activators, in which the zeta potential decreased and the contact angle increased to 102.29°.

(3) XPS analyses showed that O atoms might have been involved in the reaction of Zn^{2+} adsorbed on sphalerite in the acidic system. During adsorption, Zn^{2+} existed on the sphalerite surface in the form of a metal hydroxyl complex, which hindered Cu^{2+} adsorption on the sphalerite and made its surface hydrophilic, leading to the inhibition of sphalerite recovery. In addition, S^{2-} could effectively remove the Zn-hydroxyl complex on the sphalerite surface and promote Cu^{2+} adsorption to form a $Cu_2S{\cdot}S^0$ hydrophobic film when sphalerite−Zn^{2+} interacted with a combination of S^{2-} and Cu^{2+} activators.

Acknowledgments

The authors are grateful for the financial supports from the National Key R&D Program of China (Nos. 2018YFC0903404, 2018YFC1903400), the National Natural Science Foundation of China (No. 51974138), the Natural Science Foundation of

Jiangxi Province, China (No. 20202BABL214022), and the Research Startup Fund Project of JXUST, China (Nos. jxxjbs17032, jxxjbs19019).

References

[1] YAN Huan, CHAI Li-yuan, PENG Bing, LI Mi, PENG Ning, HOU Dong-ke. A novel method to recover zinc and iron from zinc leaching residue [J]. Minerals Engineering, 2014, 55: 103−110.

[2] MANIVANNAN S, DAVID H, ROHAN J, PIET N L L, HEINRICH A H, LUIZ H A F, ERIC D V H. Leaching and selective zinc recovery from acidic leachates of zinc metallurgical leach residues [J]. Journal of Hazardous Materials, 2017, 324: 71−82.

[3] MIN Xiao-bo, XIE Xian-de, CHAI Li-yuan, LIANG Yan-jie, LI Mi, KE Yong. Environmental availability and ecological risk assessment of heavy metals in zinc leaching residue [J]. Transactions of Nonferrous Metals Society of China, 2013, 23(1): 208−218.

[4] LI Mi, PENG Bing, CHAI Li-yuan, PENG Ning, XIE Xian-de, YAN Huan. Technological mineralogy and environmental activity of zinc leaching residue from zinc hydrometallurgical process [J]. Transactions of Nonferrous Metals Society of China, 2013, 23(5): 1480−1488.

[5] WANG Xin, SRINIVASAKANNAN C, DUAN Xin-hui, PENG Jin-hui,YANG Da-jin, JU Shao-hua. Leaching kinetics of zinc residues augmented with ultrasound [J]. Separation and Purification Technology, 2013, 115: 66−72.

[6] LIU Qing, ZHAO You-cai, ZHAO Guo-dong. Production of zinc and lead concentrates from lean oxidized zinc ores by alkaline leaching followed by two-step precipitation using sulfides [J]. Hydrometallurgy, 2011, 110(1): 79−84.

[7] MOGHADDAM J, SARRAF-MAMOORY R, ABDO-LLAHY M, YAMINIC Y. Purification of zinc ammoniacal leaching solution by cementation: Determination of optimum process conditions with experimental design by Taguchi's method [J]. Separation and Purification Technology, 2006, 51: 157−164.

[8] JIANG Guo-min, PENG Bing, LIANG Yan-jie, CHAI Li-yuan, WANG Qing-wei, LI Qing-zhu, HU Ming. Recovery of valuable metals from zinc leaching residue by sulfate roasting and water leaching [J]. Transactions of Nonferrous Metals Society of China, 2017, 27(5): 1180−1187.

[9] ŠARKA L, JURAJ L, DALIBOR M. Selective leaching of zinc from zinc ferrite with hydrochloric acid [J]. Hydrometallurgy, 2009, 95: 179−182.

[10] HAN Hai-sheng, SUN Wei, HU Yue-hu, JIA Baoliang, TANG Hong-hu. Anglesite and silver recovery from jarosite residues through roasting and sulfidization−flotation in zinc hydrometallurgy [J]. Journal of Hazardous Materials, 2014, 278: 49−54.

[11] KE Yong, CHAI Li-yuan, MIN Xiao-bo, TANG Chong-jian, CHEN Jie, WANG Yan, LIANG Yan-jie. Sulfidation of heavy-metal-containing neutralization sludge using zinc leaching residue as the sulfur source for metal recovery and stabilization [J]. Minerals Engineering, 2014, 61: 105−112.

[12] RAGHAVAN R, MOHANAN P K, PATNAIK S C. Innovative processing technique to produce zinc concentrate from zinc leach residue with simultaneous recovery of lead and silver [J]. Hydrometallurgy, 1998, 48(2): 225−237.

[13] FORNASIERO D, RALSTON J. Effect of surface oxide/hydroxide products on the collectorless flotation of copper-activated sphalerite [J]. International Journal of Mineral Processing, 2006, 78(4): 231−237.

[14] YURI M, ANTON K,YEVGENY T, ANDREY S. Interaction of sphalerite with potassium n-butyl xanthate and copper sulfate solutions studied by XPS of fast-frozen samples and zeta-potential measurement [J]. Vacuum, 2016, 125: 98−105.

[15] ANDRE R G, ANGEL G L, KATHRYN E P, ROGER S C S. The mechanism of copper activation of sphalerite [J]. Applied Surface Science, 1999, 137(1): 207−223.

[16] ALBRECHT T W J, ADDAI-MENSAH J, FORNASIERO D. Critical copper concentration in sphalerite flotation: Effect of temperature and collector [J]. International Journal of Mineral Processing, 2016, 146: 15−22.

[17] LI Jian-min, SONG Kai-wei, LIU Dian-wen, ZHNAG Xiao-lin, LAN Zhuo-yue, SUN Yun-li, WEN Shu-ming. Hydrolyzation and adsorption behaviors of SPH and SCT used as combined depressants in the selective flotation of galena from sphalerite [J]. Journal of Molecular Liquids, 2017, 231: 485−490.

[18] LIU Jian, WANG Yu, LUO De-qiang, ZENG Yong. Use of $ZnSO_4$ and SDD mixture as sphalerite depressant in copper flotation [J]. Minerals Engineering, 2018, 121: 31−38.

[19] EEl-SHALL H, AELGILLANI D, ABDEL-KHALEK N A. Role of zinc sulfate in depression of lead-activated sphalerite [J]. International Journal of Mineral Processing, 2000, 58(1): 67−75.

[20] GAO Ming-li, LIU Qi. Reexamining the functions of zinc sulfate as a selective depressant in differential sulfide flotation-The role of coagulation [J]. Journal of Colloid and Interface Science, 2006, 301(2): 523−531.

[21] WANG Han, WEN Shu-ming, HAN Guang, XU Lei, FENG Qi-heng. Activation mechanism of lead ions in the flotation of sphalerite depressed with zinc sulfate [J]. Minerals Engineering, 2020, 146: 106132.

[22] XIA L, HART B, FURLOTTE M, GINGRAS G, OLSEN C. Mechanism of sphalerite depression in an open Cu/Zn flotation separation circuit [C]//Proceedings of XXVIII International Mineral Processing Congress. Quebec, 2016.

[23] EJTEMAEI M, PLACKOWSKI C, NGUYEN A V. The effect of calcium, magnesium, and sulphate ions on the surface properties of copper activated sphalerite [J]. Minerals Engineering, 2016, 89: 42−51.

[24] NDUNA M K, LEWIS A E, NORTIER P. A model for the zeta potential of copper sulphide [J]. Colloids and Surfaces A: Physicochemical and Engineering Aspects, 2014, 441: 643−652.

[25] EJTEMAEI M, NGUYEN A V. Kinetic studies of amyl xanthate adsorption and bubble attachment to Cu-activated sphalerite and pyrite surfaces [J]. Minerals Engineering, 2017, 112: 36−42.

[26] CRUZ R, BERTRAND V, MONROY M, GONZÁLEZ I.

Effect of sulfide impurities on the reactivity of pyrite and pyritic concentrates: A multi-tool approach [J]. Applied Geochemistry, 2001, 16(7): 803−819.

[27] KLAUBER C, PARKER A, BRONSWIJK W V, WATLING H. Sulphur speciation of leached chalcopyrite surfaces as determined by X-ray photoelectron spectroscopy [J]. International Journal of Mineral Processing, 2001, 62(1): 65−94.

[28] LAAJALEHTO K, KARTIO I, SUONINEN E. XPS and SR-XPS techniques applied to sulphide mineral surfaces [J]. International Journal of Mineral Processing, 1997, 51(1): 163−170.

[29] YIN M, WU C K, LOU Y B, BURDA C, KOBERSTEIN J T, ZHU Y, O'BRIEN S. Copper oxide nanocrystals [J]. Journal of the American Chemical Society, 2005, 127(26): 9506−9511.

高浓度锌离子对酸性体系中闪锌矿可浮性的影响

邱廷省[1]，李国栋[1,2]，李晓波[1]，严华山[1]，刘 晨[1]

1. 江西理工大学 资源与环境工程学院，赣州 341000；
2. 西北矿冶研究院，白银 730900

摘 要：通过浮选实验、zeta 电位测试、接触角测量和 X 射线光电子能谱研究高浓度 Zn^{2+}对闪锌矿在酸性体系中可浮性的影响。结果表明，Zn^{2+}吸附于闪锌矿表面，且当 pH=4 和 Zn^{2+}浓度为 4×10^{-2} mol/L 时，在闪锌矿表面形成 Zn-羟基络合物。zeta 电位增加且接触角从 84.80°减小到 36.48°，从而极大地抑制闪锌矿的可浮性。当单独以 S^{2-}或 Cu^{2+}作为活化剂时，无法活化吸附 Zn^{2+}后的闪锌矿，其接触角也无明显变化；而采用 S^{2-}与 Cu^{2+}组合活化剂时，吸附 Zn^{2+}后的闪锌矿可被活化而浮选。这归因于 S^{2-}可先将闪锌矿表面的 Zn-羟基络合物消除，Cu^{2+}即可吸附在闪锌矿表面上并形成 $Cu_2S{\cdot}S^0$疏水膜。

关键词：酸性体系；高浓度锌离子；闪锌矿；浮选

(Edited by Wei-ping CHEN)